Comparative Study of *In Situ* Loaded Antibody and PEG-Fab NIPAAM Gels

Sahar Awwad[1,2*], Athmar Al-Shohani[1,2], Peng T. Khaw[2] and Steve Brocchini[1,2*]

[1]UCL School of Pharmacy, London, WC1N 1AX, UK

[2]National Institute for Health Research (NIHR) Biomedical Research Centre at Moorfields Eye Hospital NHS Foundation Trust and UCL Institute of Ophthalmology, London, EC1V 9EL, UK

Keywords: hydrogel, stimuli responsive, therapeutic protein, PEGylated protein; ocular delivery

*Corresponding authors: s.awwad@ucl.ac.uk and steve.brocchini@ucl.ac.uk

Graphical abstract

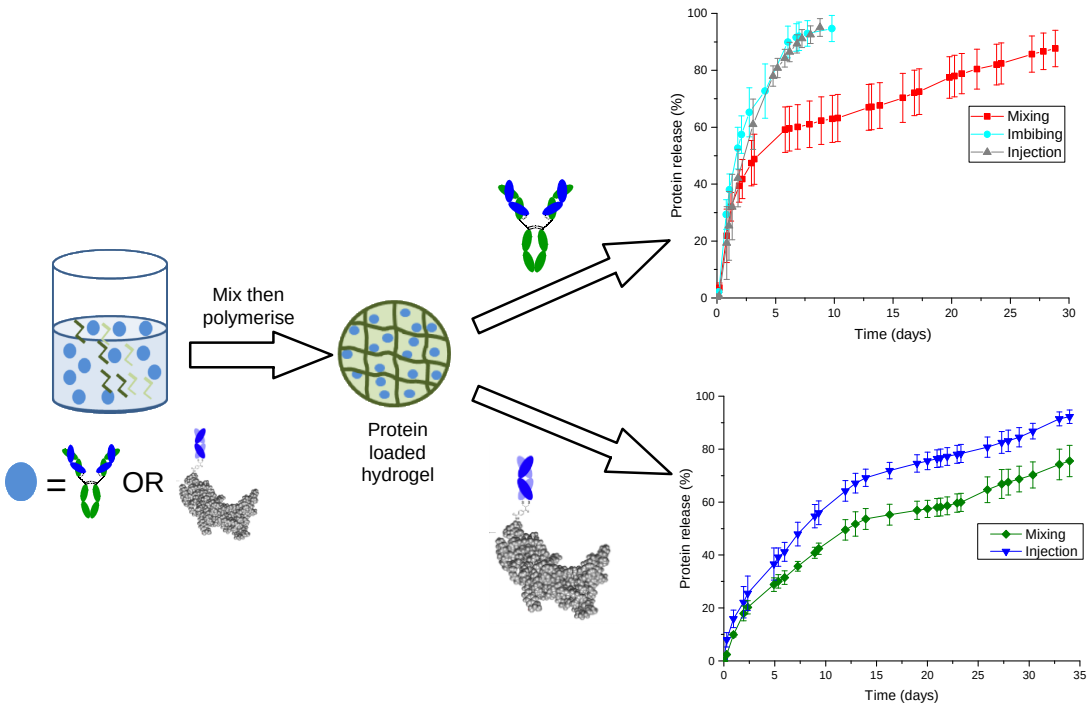

Abstract

Hydrogels can potentially prolong the release of a therapeutic protein, especially to treat blinding conditions. One challenge is to ensure the protein and hydrogel are intimately mixed by better protein entanglement within the hydrogel. *N*-isopropylacrylamide (NIPAAM) gels were optimised with PEG-diacrylate (PEGDA) crosslinker in the presence of either bevacizumab or PEG conjugated ranibizumab (PEG_{10}-Fab_{rani}). The release profiles of the hydrogels were evaluated using an outflow model of the eye, which has been previously validated for human clearance of proteins. Release kinetics of *in situ* loaded bevacizumab-NIPAAM gels displayed a prolonged bimodal release profile in PBS compared to bevacizumab loaded into a preformed NIPAAM gel. Bevacizumab release in simulated vitreous from *in situ* loaded gels was similar to bevacizumab control indicating that diffusion through the vitreous rather than from the gel was rate limiting. Ranibizumab was site-specifically PEGylated by disulfide rebridging conjugation. Prolonged and continuous release was observed with the *in situ* loaded PEG_{10}-Fab_{rani}-NIPAAM gels compared to PEG_{10}-Fab_{rani} injection (control). Compared to an unmodified protein, there is better mixing due to PEG entanglement and compatibility of PEG_{10}-Fab_{rani} within the NIPAAM-PEDGA hydrogel. These encouraging results suggest that the extended release of PEGylated proteins in the vitreous can be achieved using injectable hydrogels.

1. Introduction

Hydrogels are frequently considered as materials that can be used to prolong the duration of action of therapeutic proteins.[1] A limitation of crosslinked hydrogels is it is not possible to mix a large molecule (such as an antibody) efficiently within a pre-existing hydrogel. One strategy to address this 'mixing problem' is to form the hydrogel in the presence of the protein in solution. The high water content within the hydrogel is thought to be important for maintaining protein stability, but the high water content often results in burst release profiles for water soluble actives, such as proteins.[2] *In situ* collapsing hydrogels[3-4] have been used to avoid a 'burst' release phase and to prolong the overall drug release profile.[5-7]

Therapeutic antibodies are increasingly being used to treat blinding conditions. Antibody based medicines that bind to vascular endothelial growth factor (VEGF) are administered by intravitreal (IVT) injection to treat wet age-related macular degeneration (AMD), which is the main cause of blindness in the elderly population. While IVT injections are the best way to administer a reproducible dose of an antibody to the back of the eye,[8] clinical practice is hampered by the need for IVT injections of these medicines every 1-2 months. To better treat chronic blinding conditions, there is a need to develop ocular formulations that could maintain a therapeutic dose of a medicine in the vitreous cavity for longer periods of time.[9-13]

To this end, IVT implants for the sustained delivery of low molecular weight poorly soluble actives, e.g. corticosteroids have been clinically approved.[14-15] The formulation of analogous IVT implants utilising a protein therapeutic is limited due to protein aggregation.[16-17] Particulate associated formulations (e.g. nano- and microspheres) are widely described[18] and while there has been much research to develop these formulations for intraocular use[19], most clinically registered products are for non-ophthalmic indications and are derived from low molecular weight

molecules and peptides such as Exenatide®, Sandostatin®, Vivitrol® and Risperdal Consta®.[20-23]

Particulate formulations often use polymers (e.g. poly(lactic-co-glycolic acid) (PLGA)[24]) that must be processed using organic solvents and/or require emulsification processes. Scale up and sterilisation processes are limited because of protein stability.[1, 25-26] However particulate associated formulations of proteins for IVT injections have been described.[9, 27] Particles which are prone to aggregation or larger than 300 nm in the vitreous can scatter light to interfere with vision.[28] Particle migration to the front of the eye[9, 27] results in release of drug that simply clears from the eye with aqueous outflow. An additional risk is particulates blocking the aqueous outflow.

To avoid issues with particulates and regular IVT injection, a surgically implanted port delivery system for ranibizumab is currently in clinical trials.[29] Ranibizumab is an antibody Fab that is clinically approved to treat AMD and is typically administered monthly. The implant port delivery system would be refilled with ranibizumab once every four months. To avoid potential implantation issues (e.g. foreign body response, ocular infection) and the limitations of free particulates,[30] hydrogels[17, 31-32] including collapsible gel systems[5] have emerged as potential platforms for extending the duration of action of therapeutic proteins.

Responsive hydrogels that collapse in physiological conditions can entrap a therapeutic protein,[33-35] so that if protein loaded hydrogel can be injected into the posterior cavity of the eye, the hydrogel could then collapse to then act as a depot to prolong the release of the protein. Design of a collapsible hydrogel should account for the presence of less water to avoid protein degradation. Thermoresponsive polymers derived from *N*-isopropylacylamide (NIPAAM) have been utilised in many drug delivery and tissue engineering studies.[36] NIPAAM has been shown to display no retinal toxicity *in vivo*[37] although formulations derived entirely from NIPAAM are not expected to be resorbable. When NIPAAM is prepared in the presence of a

small amount of a di-acrylate crosslinker (e.g. polyethylene (glycol) diacrylate (PEGDA)), a NIPAAM hydrogel will form. To ensure that there is good protein encapsulation during hydrogel formation, polymerisation bond forming reactions must be orthongonal to avoid reaction with the protein. For example thiol derived crosslinks[17] that could leave residual thiol would be expected to undergo disulfide scrambling reactions with an entrapped therapeutic protein.

To address the protein mixing challenge in hydrogels, we prepared NIPAAM hydrogels in the presence of bevacizumab and PEGylated ranibizumab to compare the release profiles of the proteins from the collapsed NIPAAM hydrogel. The *in vitro* release profiles of these protein loaded NIPAAM hydrogels were studied in an *in vitro* outflow model called the PK-Eye.[38-40] This model has been shown to estimate human clearance times of protein therapeutics from the back of the eye. The PK-Eye reduces animal use during preclinical development and avoids the intractable problems associated with the development of anti-drug antibodies (ADAs).

2. Results and Discussion

2.1 Bevacizumab loaded NIPAAM hydrogel preparation and characterisation

The relative molar amounts of PEGDA to NIPAAM ranged from 1.8 to 9.1% to evaluate crosslink densities to prepare a hydrogel that could potentially be injected prior to its collapse. The injectability of the gels were determined qualitatively by ensuring they could pass with little resistance through a 23 G needle for these studies. Gels prepared using 4 and 8 µL (6.4 and 13 µM respectively) of PEGDA were easily injectable. Higher amounts of PEGDA (i.e. 12 to 20 µL) crosslinker produced gels that were less easily injectable. In a similar study with NIPAAM and PEGDA, ~8 µM of PEGDA was found to be an optimal crosslinker concentration to ensure ease of injection through slightly smaller gauge needles (<27-30 G).[41]

The NIPAAM hydrogels were characterised to further aid the selection of the crosslink density to be used to evaluate bevacizumab entrapment (Figure 1A-C, left

column). DSC analysis indicated that the VPTT varied only slightly in the range 34.3 ± 0.2 to 36.2 ± 0.2°C for PEGDA amounts from 4 to 15 µL (Figure 1A, left column). These VPTT values were only slightly higher than other NIPAAM-PEGDA hydrogels (33°C) that have been reported. As expected the swelling ratio (SR) decreased with increased levels of the PEGDA crosslinker at 25°C (Figure 1B, left column). After gel collapse at 37°C, the overall SR decreased at low relative crosslink density (Figure 1B, left column) where collapse appeared more complete. The percentage water retention (WR%) after gel collapse (37˚C) indicated that more water was expelled after gel collapse at low relative crosslink density (Figure 1C, left column), which was consistent with the SR.

The amount of water that is associated within a hydrogel can be influenced by polymer composition, crosslink density and protein loading. Decreased hydrogel swelling occurs with an increase in crosslink density (Figure 1C, left column). Although many diacrylate crosslinkers are available, PEGDA was selected because it is known as a pore-forming agent when used for hydrogel preparation.[34] The hydration and the steric shielding properties of PEG may be important to form a more porous hydrogel structure[42] and to eventually encourage PEG entanglement with a PEGylated protein. PEGDA (Mn 700) was selected because it was thought the molecular weight was large enough to display PEG steric shielding needed to produce a porous hydrogel. PEGDA (Mn 700) was also thought to be a low enough molecular weight to maintain a physiologically relevant NIPAAM LCST. Increased PEG molecular weights give hydrogels a higher temperature transition point.[42]

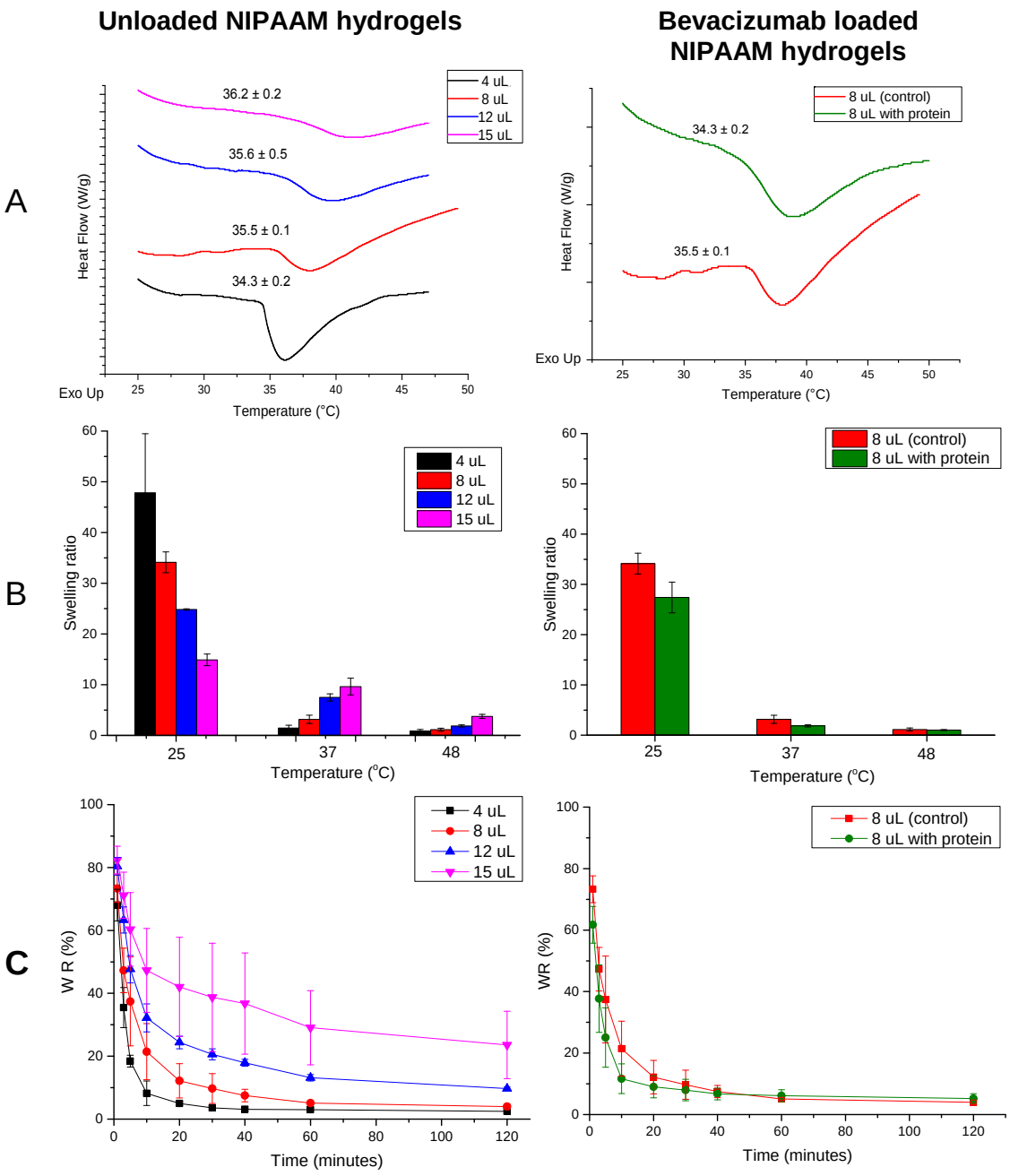

Figure 1. Characterisation of unloaded (control, left column) and bevacizumab (right column) loaded NIPAAM hydrogels. (A) Volume phase transition temperature (VPTT) with DSC at 2°C/min from 20 to 50°C; (B) swelling ratio (SR) measured at 25, 37 and 48°C and (C) water retention percentage (WR%) at 37°C. All data presented was done in triplicate (n=3) and presented as its mean and standard deviation (± STD).

2.2 Bevacizumab dose determination

Bevacizumab is not licensed for IVT injection and has been used as a substitute for ranibizumab, which is a Fab that also binds to VEGF and is clinically registered to treat AMD.[43-44] The ophthalmic use of bevacizumab has been driven by cost because ranibizumab is considerably more expensive per dose. The clinical IVT dose of bevacizumab is 1.25 mg which is the amount obtained from 50 µL of bevacizumab (25 mg/mL) that is formulated for use in oncology.[45]

Prior to loading bevacizumab into the NIPAAM gel, three doses of bevacizumab (Figure 2) were evaluated using the PK-Eye to determine clearance times. The PK-Eye is a two compartment, aqueous outflow model scaled to the eye that has been shown to estimate the human clearance times of therapeutic proteins from the back of the eye.[39]. Novel formulations of protein therapeutics and long acting implants can be optimised and *in vitro in vivo* correlations (IVIVCs) elucidated.[38, 40] *In vitro* models are widely used in preclinical development designed to determine intraocular release kinetics of therapeutic proteins. Aqueous outflow (2.0-2.5 µL/min) is the main cause of mass trasfer within the eye.[46-50] In research, little has been reported to develop an *in vitro* model that accounts for the aqueous flow to estimate clearance times for molecules that exit the eye predominantly via the anterior route such as therapeutic proteins. Early preclinical development times can be accelerated until an optimised formulation is obtained. This avoids the unnecessary use of animals, which generally (i) carry the risk of developing ADAs[51-55] and (ii) do not account for many differences anatomical differences that exist between animal and human eyes.[56-57] A significant amount of effort is necessary to obtain protein stability and functional data from animal models. Protein stability may be lost in long acting formulations designed for the vitreous cavity. One potential advantage of the PK-Eye is the ease to evaluate protein properties such as stability and functionality. Animals can quickly develop ADAs, which is an intractable problem

that negatively impacts the preclinical development of long lasting dosage forms or devices for ocular use (Figures S1-S3).

The fitting model in Origin showed a first order release kinetics with a mono-exponential decay. A 1.25 mg dose of bevacizumab displayed a *k* value of 0.068 ± 0.0004 days^{-1} and an estimated outflow clearance half-life ($t_{1/2}$) of 10.1 ± 0.7 days using simulated vitreous in the PK-Eye model (Figure 2A), which is comparable to what is observed in humans (6.7-10.0 days).[58-61] The bevacizumab dose was increased to 2.5 and 5.0 mg and clearance $t_{1/2}$ times of 15.4 ± 0.7 and 18.3 ± 1.1 days were observed respectively using simulated vitreous in the PK-Eye (Figure 2B).

An ocular hydrogel formulation of a therapeutic protein requires the protein to first diffuse from the gel followed then diffuse from the vitreous cavity. In an animal model, the prolonged exposure to a protein therapeutic would be expected to generate ADAs when using a human derived protein. Understanding the effects of the hydrogel to optimise a formulation can be more efficiently studied in a relevant non-animal model, such as the one used in this study. Using this strategy is more efficient for developing other dosage forms (e.g. oral)..

Considering the amount of bevacizumab to incorporate into a NIPAAM hydrogel was important. Adding more mass of bevacizumab (or any drug) into a final dosage form is a strategy that can increase the number of clearance $t_{1/2}$s before a sub-therapeutic concentration is reached. This strategy exploits a therapeutic tail that is possible for potent molecules. For example, aflibercept is an antibody fusion protein that also binds to VEGF for the treatment of AMD. Aflibercept is administered by IVT injection about every 2 months.[62] More aflibercept on a molar basis is in the IVT injection volume than the other antibody based drugs that are dosed once monthly to treat AMD (i.e. bevacizumab and ranibizumab).

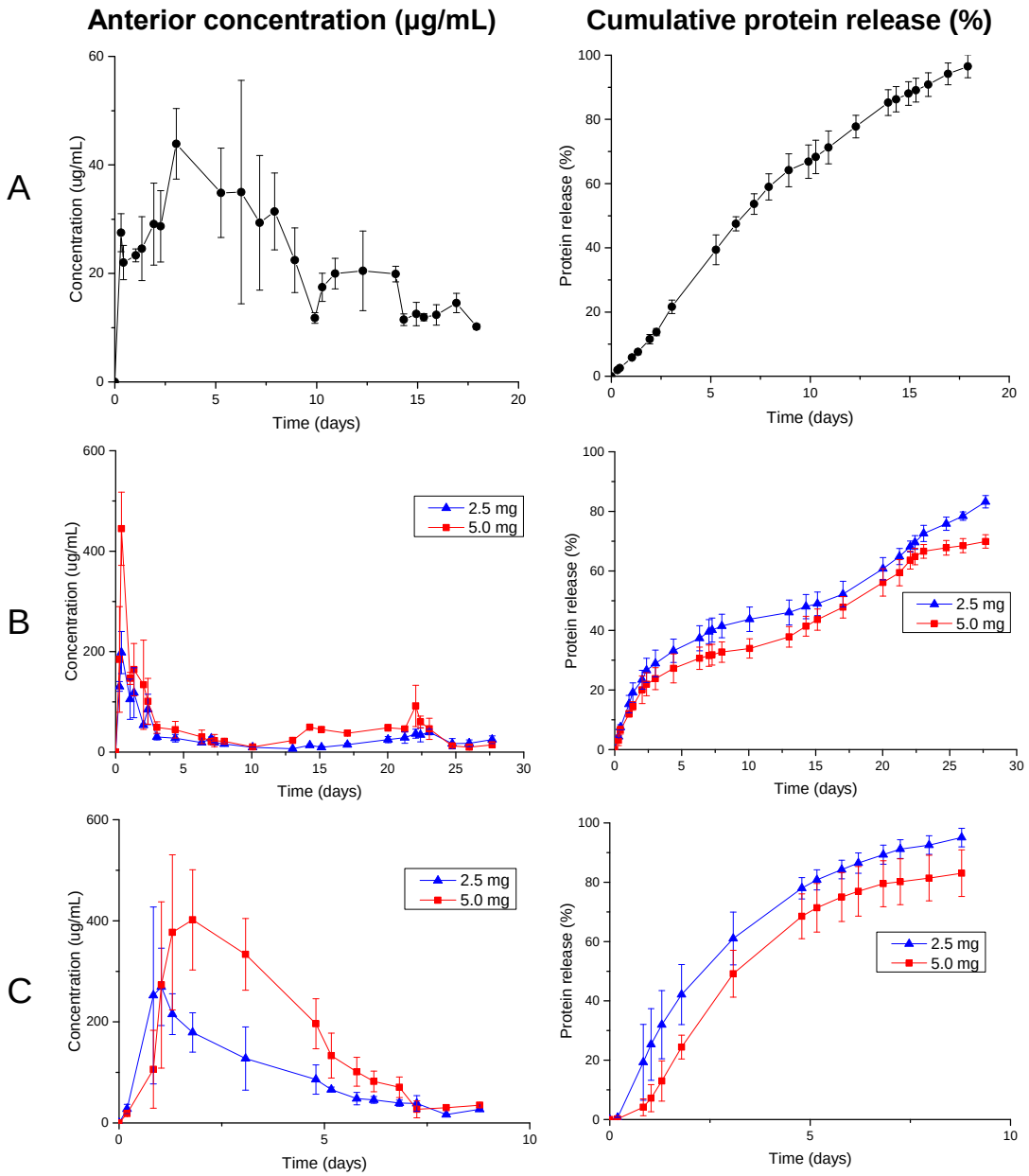

Figure 2. *In vitro* release profiles of different bevacizumab doses at 37°C to determine the bevacizumab pNIPAAM loading. **(A)** Clinical dose of bevacizumab (1.25 mg) in simulated vitreous. Larger doses (2.5 and 5.0 mg) in **(B)** simulated vitreous and (**C)** PBS, pH 7.4. All data obtained by HPLC (280 nm) in triplicate (n=3) and presented as its mean and standard deviation (± STD).

Although aflibercept is dosed less frequently than either ranibizumab or bevacizumab, this is not because there is any significant increase in the vitreal $t_{1/2}$ of aflibercept compared to either ranibizumab or bevacizumab. A strategy based simply on having more bevacizumab in a 50 µL IVT injection volume would not be expected to dramatically increase the duration of action of bevacizumab to more than 2 months, but loading a larger dose of bevacizumab into a gel may offer the

opportunity to increase the duration of action of an injectable gel-based form of bevacizumab.

Dose escalation was also conducted using PBS in the vitreous cavity of the PK-Eye. PBS was then used instead of simulated vitreous in the posterior cavity of the PK-Eye to compare and to observe relative clearance $t_{1/2}$s more quickly. The 2.5 and 5.0 mg bevacizumab doses displayed a $t_{1/2}$ of 2.4 ± 0.8 and 3.5 ± 0.7 days respectively (Figure 2C). The percentage of the protein that cleared from the posterior cavity of the PK-Eye using PBS by day 9 was 95.1 ± 3.1 and 83.0 ± 7.9 % for the 2.5 and 5.0 mg doses respectively. For comparison, a $t_{1/2}$ of 1.2 ± 0.1 days and a protein release of 93.6 ± 7.6% was observed for the clearance of the clinical dose (1.25 mg) of bevacizumab with PBS in the PK-Eye.[39]

The same strategy to add as more drug to a formulation is also seen with subcutaneous drugs (SC), for example, the initial formulation of glatiramer was a 20.0 mg dose for daily SC administration. The next generation formulation of glatiramer was 40.0 mg dose in the same 1.0 mL volume for 3 times weekly administration. With more glatiramer in the 40.0 mg dose, it took longer for all of the drug to diffuse into circulation and the duration of action of glatiramer was increased.

2.3 Loading and characterisation of bevacizumab-NIPAAM hydrogel

It is not possible to mix a large molecule such as a therapeutic protein efficiently with a preformed hydrogel. A strategy to address this ‘mixing problem’ is to form the gel while in the presence of the protein in solution. To prepare the loaded gels, bevacizumab (2.5 mg, 100 µL) was mixed with the monomer, initiator and 4, 8 and 12 µL PEGDA. SEM images (bottom panel, Figure 3) indicate that freeze-dried bevacizumab-NIPAAM hydrogels have a similar morphology to the NIPAAM gels prepared without antibody (top panel, Figure 3). The bevacizumab loaded gel prepared using 8 µL PEGDA (beva-8µL gel) was easily injectable while also appearing to have an intact porous structure.

The beva-8μL PEGDA gel displayed a similar VPTT value (Figure 1A, 34.3 ± 0.2°C) to the gel without bevacizumab that was prepared with the same amount of PEGDA. The SR of the beva-8μL PEGDA gel was slightly higher at 25°C than the unloaded NIPAAM gel ($p<0.05$), while at 37 and 48°C there was little difference in the SR between loaded and unloaded gels (Figure 1B). The WR of the beva-8μL PEGDA gel was the same as the unloaded NIPAAM gel (Figure 1C). It appears that the VPTT and the swelling properties of the NIPAAM gel do not significantly change in the presence of bevacizumab (2.5 mg) loading.

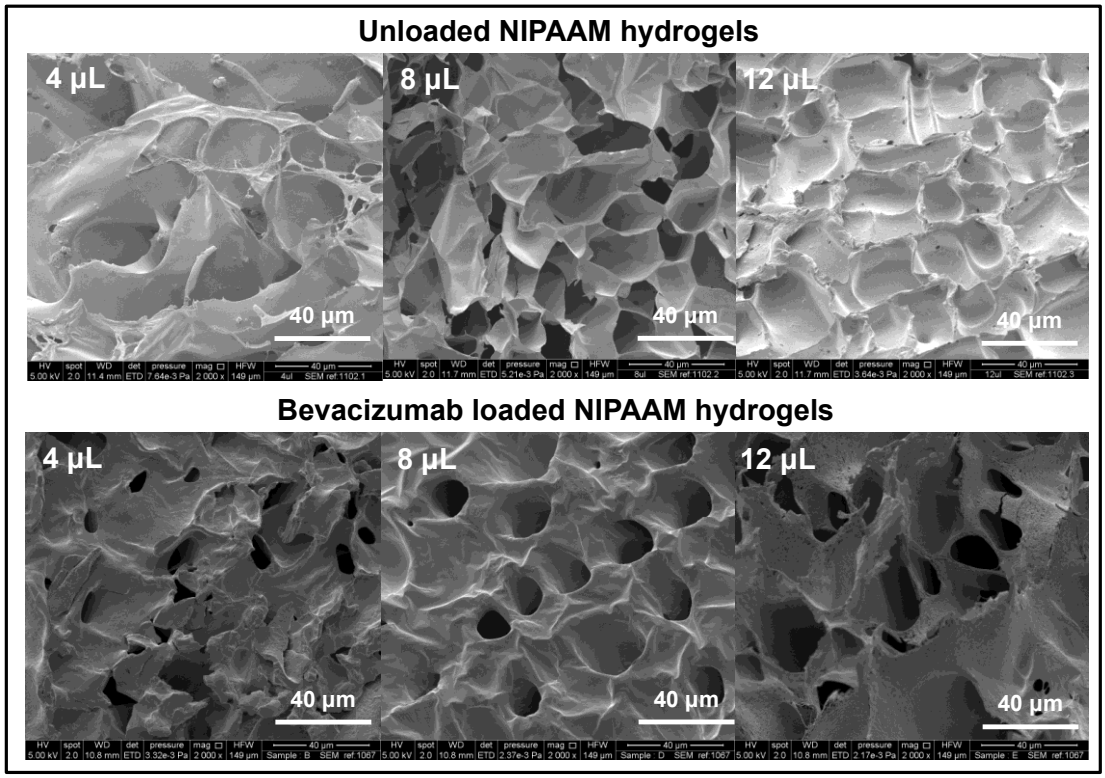

Figure 3. Scanning electron microscopy (SEM) images of NIPAAM gels (40 μm scale). **(Top panel)** unloaded and **(bottom panel)** bevacizumab (2.5 mg) loaded NIPAAM hydrogels prepared PEGDA. Each sample was repeated in triplicate (n=3).

A decreased SR was expected with increased crosslink density due to greater restriction of NIPAAM polymer chain mobility.[63] The hydrophilicity of PEGDA may result in a reduction of the NIPAAM hydrophobic interactions, which could also contribute to the reduction of SR with PEGDA incorporation.[64-66] However greater SR was observed for the more densely crosslinked hydrogel (e.g. 12 μL PEGDA; Figure 1B). The SR of the beva-8μL PEGDA gel was significantly different to the

unloaded gel ($p<0.05$) at 25°C; but not significantly different ($p>0.05$) at 37 and 48°C. As expected the decreased SR at 37 and 48°C was due to NIPAAM collapse and was not affected by the presence of bevacizumab.[33] Deswelling starts at the gel surface due to the free mobile nature of the surface and the diffusion of the crosslinked polymer network in water.[67] During gel collapse, some of entrapped protein can be released from the hydrogel.[63] The WR of beva-8μL PEGDA was similar to the unloaded gel ($p>0.05$). It was necessary to determine the hydrogel properties in the presence and absence of bevacizumab to ensure antibody loading did not adversely affect gel collapse properties.

2.4 Bevacizumab loaded NIPAAM gel release profile

Clearance profiles for the *in situ* loaded bevacizumab gels prepared were first determined using PBS in the PK-Eye (Figure 4A). The $t_{1/2}$ of bevacizumab was 2.0 ± 0.01, 3.7 ± 1.2 and 2.6 ± 0.03 days with the respective PEGDA amounts of 4, 8 and 12 μL. Bimodal release profiles comprised of a first burst phase (60% of bevacizumab being cleared after 5 days) followed by a slower prolonged release phase are often observed with hydrogels.[34] Crosslink density appeared to have more impact on the second, slower phase of release with 74.2 ± 3.5, 87.6 ± 6.4 and 95.8 ± 2.3% of the bevacizumab being released after a month with 4, 8 and 12 μL PEGDA respectively (Figure 4A). The *in situ* loaded beva-8μL PEGDA gel appeared to have a more prolonged release profile than was observed for either (i) the simple soaking or incubation of bevacizumab with a preformed gel NIPAAM hydrogel or (ii) bevacizumab injection without the hydrogel (Figure 4B).

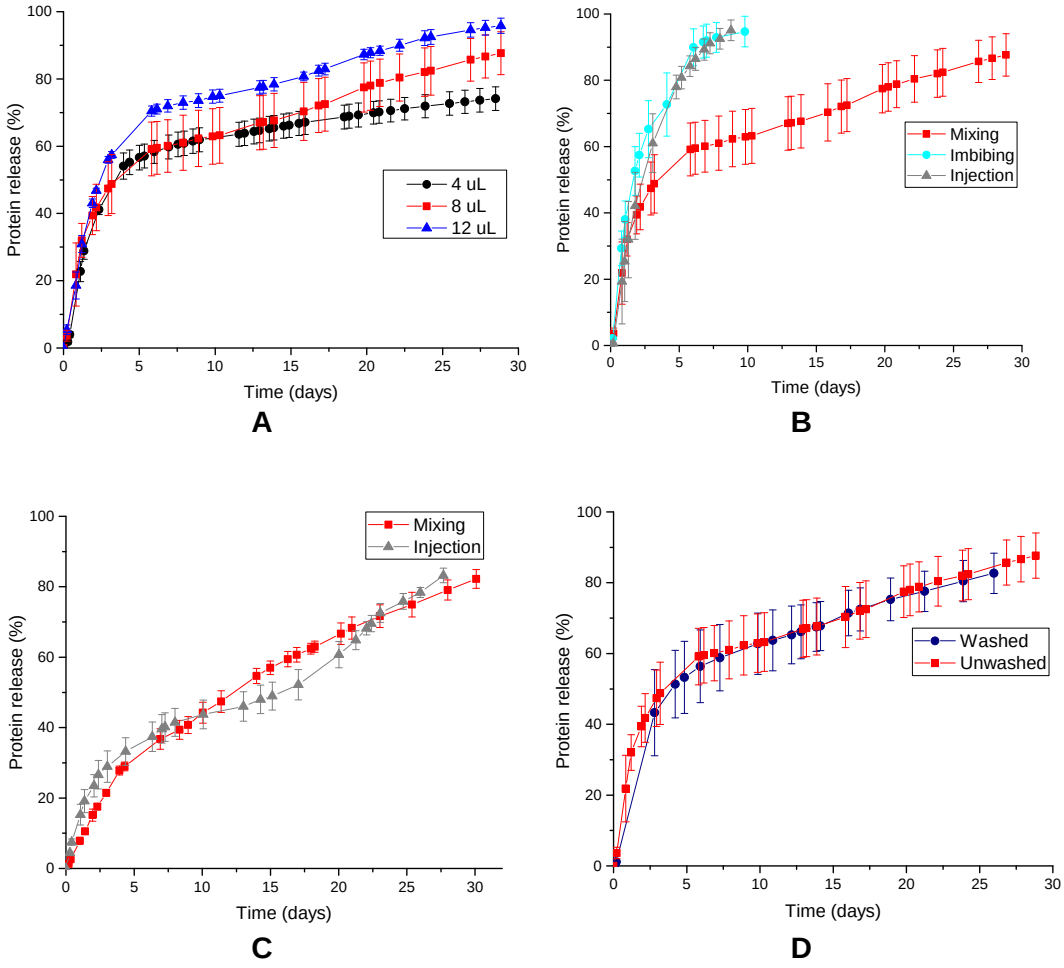

Figure 4. Release profiles of bevacizumab (2.5 mg) loaded NIPAAM hydrogels released from either PBS or simulated vitreous in the PK-Eye at 37°C. **(A)** Bevacizumab and NIPAAM mixed *in-situ* then polymerised in the presence of different amounts of PEGDA crosslinker followed by release in PBS, **(B)** comparative release profiles in PBS of bevacizumab injection and bevacizumab NIPAAM loaded hydrogels prepared by hydrogel imbibition of a preformed gel and by *in situ* mixing during hydrogel formation crosslinked with PEGDA (8.0 μL), **(C)** bevacizumab-*in situ* mixed NIPAAM hydrogel (8 μL PEGDA) compared to control (injection, no hydrogel) released from simulated vitreous and **(D)** washed versus unwashed bevacizumab from *in situ* mixed NIPAAM hydrogels released using PBS for release in the PK-Eye. All data obtained by HPLC (280 nm) presented was done in triplicate (n=3) and presented as its mean and standard deviation (± STD).

The incubation of bevacizumab with the preformed hydrogel resulted in 52.6 ± 7.3 and 92.0 ± 5.0% of the release of antibody after 2 and 7 days respectively. About 100.6 ± 3.4% of bevacizumab was released by day 17. These results were not surprising, as the gel tends to swell and completely expel the protein. The protein was not entangled within the hydrogel network. An outflow $t_{1/2}$ of 1.9 ± 0.3 days was observed (Figure 4B) during the first rapid phase of the release.

Although the use of PBS in the PK-Eye can estimate the clearance time for patients that have had a vitrectomy,[39] most patients will have their own vitreous. There was little difference in the release profiles when simulated vitreous was used with the beva-8μL gel or by simple injection of the antibody alone (Figure 4C). The viscosity of the simulated vitreous slowed the diffusion of bevacizumab once it was released from the gel compared to PBS. The rate of bevacizumab clearance during the first burst phase from the beva-8μL gel was dampened due to the reduced diffusion of the antibody from the viscous simulated vitreous within the PK-Eye. The difference observed using PBS and simulated vitreous in a relevant *in vitro* release model illustrate how it is possible to deconvolute characteristics of a release profile from a candidate drug delivery system.

The viscosity and microstructure of the vitreous can vary between patients, and often the vitreous is less viscous in the elderly.[68] The $t_{1/2}$ of bevacizumab in a victrectomised human eye from a single patient is 0.7 days,[69] so early knowledge in preclinical development about the difference in IVT release profiles that can range from being non-viscous to viscous has clinical implications. Many patients that require IVT injection of anti-VEGF therapeutic proteins have complex ocular conditions that may affect the vitreous properties or retinal permeation (e.g. torn inner limiting membrane) and may impact the clearance times of therapeutic proteins. For example, bevacizumab can have mean values in humans that vary from 4.9 to 10 days.[58-61, 69] While a bevacizumab loaded gel would have more potential for patients that have a vitreous with reduced viscosity, there may be less benefit for the larger population of patients that would be expected to have a more intact vitreous.

A post-polymerisation wash step as described elsewhere[34, 35] to remove leachable NIPAAM monomer and oligomeric species was examined using the beva-8μL PEDGA gel. Upon polymerisation the gel was washed using several vials of PBS (4 ×, 5.0 mL each, 20 mL total) with gentle shaking/swirling for 5-10 mins for

each wash cycle. A total of 28% of the antibody was lost after the washing process. To compensate for the antibody losses due to washing, a larger amount of the washed beva-8μL PEDGA gel (125 μL) was evaluated in the PK-Eye using PBS and gave a similar release profile as observed for a 2.5 mg dose of the beva-8μL PEDGA gel (100 μL) that had not been washed (Figure 4D).

2.5 Preparation of PEG_{10}-Fab_{rani} loaded NIPAAM gel

Conjugation of poly(ethylene glycol) (PEG) to an antibody fragment was then examined because increased entanglement of the PEG molecules within the hydrogel could result in a longer diffusion time for the PEGylated protein from the hydrogel than an unmodified protein. Although double network gels are prepared by polymerising different macromolecules together, entanglement is important for the increased interaction between the two macromolecules.[70]

The size of PEGylated proteins are dominated by the presence of the PEG that is conjugated to the protein.[71-74] PEG is a random coil polymer with an extended conformation in solution.[74] Proteins are often globular, more ordered and are smaller in size in solution than PEG, so protein entanglement would be expected to be less than what is possible for PEG. It was expected that if the NIPAAM monomer and PEGDA crosslinker were polymerised in the presence of PEG in solution, that better PEG entanglement would be achieved than the analogous polymerisation in the presence of the unmodified antibody. It was thought that PEG would form an interpenetrating polymer network (IPN)[75] with the PEGDA-NIPAAM network, which would result in slower diffusion of a PEGylated protein from the PEGDA crosslinked NIPAAM network than the unmodified protein (that is unable to become entangled in the hydrogel network). There would be better compatibility between the PEGDA crosslinked NIPAAM and PEG compared to the unmodified protein. Greater polymer-polymer compatibility would be expected to contribute to better mixing of the PEGDA-NIPAAM and the Fab conjugated PEG chain.

PEGylating a full length antibody (PEG-IgG) may better entrap the antibody within a NIPAAM gel network. Although it is conceivable that a PEGylated antibody could have potential in the eye because the large solution structure of PEG would potentially further slow antibody diffusion in the vitreous to prolong clearance,[76-77] we decided to examine a PEGylated Fab (PEG-Fab) within the PEGDA-NIPAAM gel. Ranibizumab is a potent anti-VEGF drug that still maintains much of its binding affinity, especially at a low dissociation rate when PEGylated site-specifically.[78] It would be possible to more effectively load a gel with a higher mole fraction of PEG-Fab than a PEG-IgG. PEGylated Fabs are used clinically, for example certolizumab pegol is a clinically used PEGylated Fab´ targeted to TNF-α which is used systemically.[79]

One desirable design criterion for any IVT drug delivery strategy is that once a therapeutic protein clears from the eye into the blood stream, that it then clears quickly from the body. PEG-Fab would be expected to clear more quickly from circulation than PEG-IgG. A PEGylated Fab has recently been studied after IVT administration to rabbits[80] and significant increases in $t_{1/2}$ were observed with an increase in PEG molecular weight as compared to the unmodified protein. Clearance $t_{1/2}$ times increase as the diffusivity of a molecule decreases within the vitreous.[76, 80] Larger molecules in solution diffuse more slowly with $t_{1/2}$ being dependent on the hydrodynamic radius in solution.[77]

We decided to used a 10 kDa PEG for Fab modification as it would be expected that once a PEG_{10}-Fab clears from the eye that it then clear quickly from circulation. Ranibizumab (Fab_{rani}) was selected for these studies because this Fab is clinically registered and we have studied the PEGylation of this Fab.[78] We utilised disulfide bridging PEGylation (Figure 5A-C) to site-specifically PEGylate Fab_{rani}.[81-83] PEG_{10}-Fab_{rani} was obtained after pooling franctions from ion exchange chromatography (IEX) (Figure 5D).

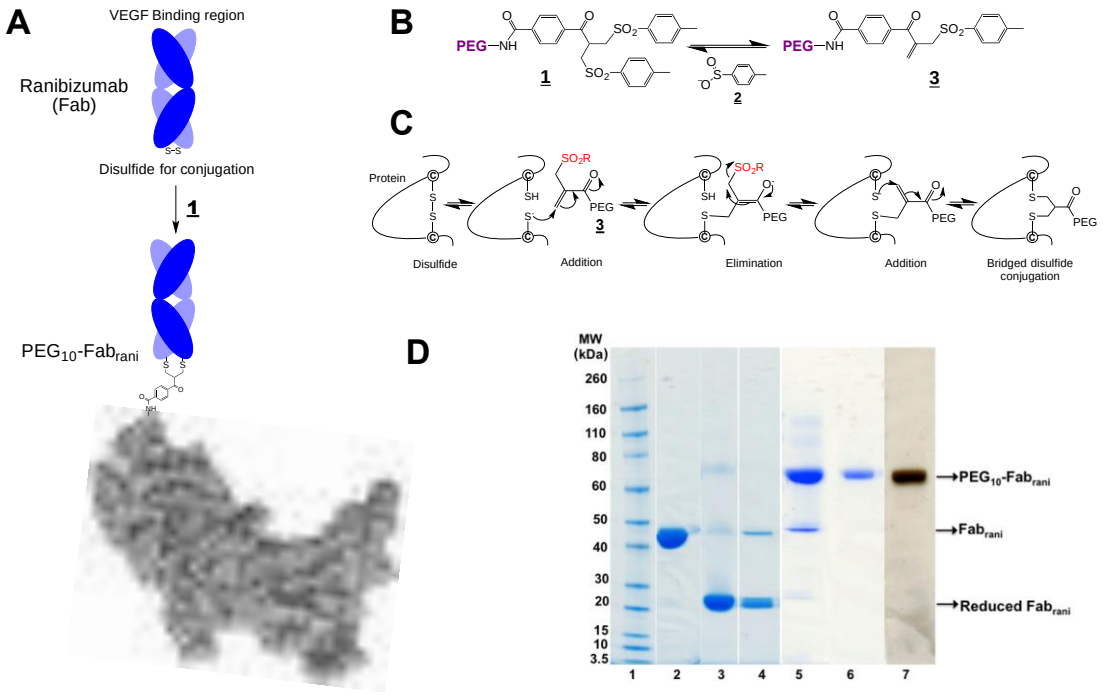

Figure 5. (A) Preparation of PEG_{10}-Fab_{rani} from the conjugation of ranibizumab with PEG *bis*-sulfone **1** derived from 10 kDa PEG precursor. **(B)** Disulfide bridging PEG conjugating reagents **1** undergo elimination of toluene sulfinic acid **2** to generate the PEG *mono*-sulfone **3** which then undergo conjugation with a reduced native accessible disulfide in a protein. PEG *bis*-sulfone reagents **1** can be prepared using different PEG molecular weights and with different polymers.[82] The *mono*-sulfones **3** are latently crossed functionalised reagents capable of sequential and interactive addition-elimination reactions capable of *bis*-alkylation. **(C)** The mechanism for conjugation first shows the cysteine thiols are liberated by reduction (e.g. TCEP[84] or DTT) and then conjugation involves *(i)* a first thiol addition to the *mono*-sulfone reagent **3**, *(ii)* sulphinic acid **2** elimination to generate a second double bond in the reagent which is then followed by *(iii)* addition of the second thiol in from the original disulfide to give the bridged conjugate. **(D)** SDS-PAGE for the preparation of PEG_{10}-Fab_{rani}. Novex Bis-Tris 4-12% gel stained with Coomassie blue (Lanes 1-5 and 8), barium iodide (Lanes 6-7) and silver stain (Lane 9). *Lane 1*: protein standard marker, *Lane 2*: Fab_{rani}, *Lane 3*: Reduced Fab_{rani} (5 mM DTT, before PD-10), *Lane 4*: Reduced Fab_{rani} (after PD-10), *Lanes 5 and 6*: PEG_{10}-Fab_{rani} after conjugation with PEG_{10}-*bis* sulfone **1** (before IEX), *Lane 7*: PEG_{10}-*bis* sulfone **1** in pH 7.6, *Lane 8:* A fraction at ~16 mins shows a fraction of PEG_{10}-Fab_{rani} and *Lane 9*: Pooled and concentrated fractions of PEG_{10}-Fab_{rani}. Note that PEG migrates to about twice its molecular weight compared to marker proteins, so the band at 70 kDa is consistent with the formation of PEG_{10}-Fab_{rani}.

A longer mixing time (3-4 hours) was conducted with PEG_{10}-Fab_{rani}, NIPAAM monomer, PEGDA, APS and TEMED to ensure gel formation occurs and to avoid precipitation. No gel was observed with a shorter mixing time (10 mins) as compared to bevacizumab loaded NIPAAM gels. The mixture was seen to 'crash out' of solution or did not polymerise at all resulting in a liquid consistency instead.

2.6 Release profile of PEG_{10}-Fab_{rani} loaded NIPAAM gel

The release profile of the PEG_{10}-Fab_{rani} (1.0 mg in 100 µL) injection alone displayed a $t_{1/2}$ of 9.7 ± 1.3 and 16.7 ± 1.9 days in PBS and simulated vitreous respectively (Figure 6A). Ranibizumab alone (0.5 mg, 50 µL) has previously been shown to have a $t_{1/2}$ of 1.5 ± 0.6 and 8.0 ± 3.1 days in PBS and simulated vitreous respectively,[39] the latter being similar to human *in vivo* data (7.2[85] and 9.0[86] days).

Pegaptanib (Macugen®) is a PEG-aptamer conjugated to a branched PEG (40 kDa total PEG molecular weight). It was the first approved anti-VEGF treatment for IVT injection.[87] The clinical dose of pegaptanib (0.3 mg) displays a $t_{1/2}$ of 7-8 days in humans.[88] Increasing the dose of pegaptanib by 10 times to 3.0 mg moderately increases the $t_{1/2}$ to 10 (± 4). The $t_{1/2}$ of 9.7 ± 1.3 days for PEG_{10}-Fab_{rani} is comparable to the human $t_{1/2}$ of pegaptanib, so the PEG_{10}-Fab_{rani} loaded NIPAAM hydrogel was evaluated using PBS in the PK-Eye. The $t_{1/2}$ of PEG_{10}-Fab_{rani} (2.0 mg, 200 µL) from the NIPAAM gel was 15.1 ± 0.6 days which is significantly longer ($p<0.05$) than the $t_{1/2}$ (9.9 ± 1.1 days) of an injection of PEG_{10}-Fab_{rani} of the same dose (Figure 6B). The amount of the PEG_{10}-Fab_{rani} cleared by day 33 was 75.5 ± 5.9 and 92.3 ± 2.5% from the NIPAAM hydrogel and injection respectively.

When considering the *in situ* loaded PEG_{10}-Fab_{rani} gel (Figure 6B), the clearance time was longer than for the release of PEG_{10}-Fab_{rani} alone. However, the profile for the clearance of the *in situ* loaded PEG_{10}-Fab_{rani} NIPAAM gel in PBS was the same as PEG_{10}-Fab_{rani} alone from both PBS and simulated vitreous. There was no burst phase for the release of PEG_{10}-Fab_{rani} from the NIPAAM gel as there was for bevacizumab from the NIPAAM gel. In contrast to the analogous release of bevacizumab, release of PEG_{10}-Fab_{rani} from the NIPAAM gel was significantly slower than the release of PEG_{10}-Fab_{rani} without having been loaded into the gel, indicating that there was better mixing of the PEGylated Fab within the gel than there was for the antibody.

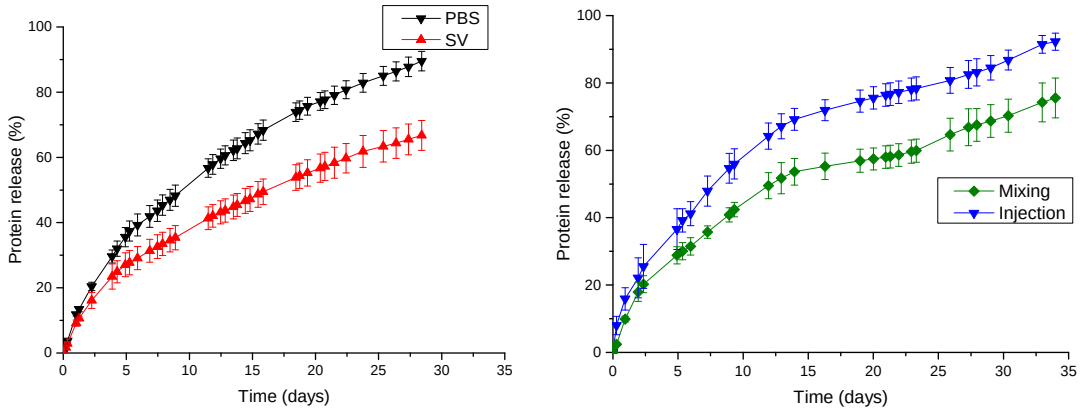

A **B**

Figure 6. Cumulative release profiles of PEG_{10}-Fab_{rani} from the PK-Eye at 37°C; **(A)** 1.0 mg in PBS (pH 7.4) and simulated vitreous (SV) and **(B)** 2.0 mg mixed *in situ* into the hydrogel and injection without the hydrogel in PBS (pH 7.4). All data obtained by HPLC (280 nm) in triplicate (n=3) and presented as its mean and standard deviation (± STD).

3. Conclusion

To promote good mixing that is required to load a protein into a hydrogel so that drug action can be prolonged in the back of the eye, thermoresponsive NIPAAM hydrogels were prepared in the presence of either bevacizumab or PEGylated ranibizumab. The *in situ* loaded bevacizumab-NIPAAM hydrogels displayed a bimodal and prolonged release profile compared to the release of bevacizumab from a preformed NIPAAM gel that had been loaded by prior incubation with a bevacizumab solution. The gel that was loaded by incubation had a similar release profile as bevacizumab, which had been administered in the absence of the hydrogel. Using simulated vitreous, the *in situ* loaded bevacizumab NIPAAM gel displayed a similar release profile as free bevacizumab.

It was found that PEG_{10}-Fab_{rani} displayed a similar $t_{1/2}$ to that of pegaptanib in humans using PBS in the PK-Eye. The *in situ* mixed NIPAAM loaded PEG_{10}-Fab_{rani} displayed a longer clearance $t_{1/2}$ than free PEG_{10}-Fab_{rani} while following a similar release profile. These results suggest that PEG entanglement within the PEGDA-NIPAAM hydrogel results in better mixing of PEG_{10}-Fab_{rani} than it is possible for unmodified bevacizumab. Prolonging the release of a protein for IVT use from a

hydrogel requires that the protein and hydrogel are optimally mixed and evaluated in a realistic *in vitro* model of the eye based on aqueous outflow.

4. Experimental Section

Materials

Ranibizumab (Lucentis®, 10.0 mg/mL) and bevacizumab (Avastin® 25.0 mg/mL) from Genentech, South San Francisco, California were supplied from the leftover syringes and purchased from Moorfields Eye Hospital respectively. Protein integrity and stability were previously monitored by sodium dodecyl sulfate polyacrylamide gel electrophoresis (SDS-PAGE), size exclusion chromatography (SEC) and surface plasmon resonance (SPR) with BIAcore. *N*-isopropylacrylamide (NIPAAM, 97%), *N*,*N*,*N*′,*N*′-tetramethylethylenediamine (TEMED, ~99%), ammonium persulfate (APS), poly(ethylene glycol) diacrylate (PEGDA, Mn: 700), DL-dithiothreitol (DTT), sodium triacetoxyborohydride (STAB), dimethyl sulfoxide (DMSO), InstantBlue™, poly(ethylene glycol) mono-amine (10 kDa), anhydrous toluene (99.8%), dichloromethane (DCM), 4-dimethyl amino pyridine (DMAP, 99+ %) and human vascular endothelial growth factor ($hVEGF_{165}$) were purchased by Sigma-Aldrich (Gillingham, Dorset, UK). Ethylenediaminetetraacetic acid dihydrate (EDTA), acetone and sodium chloride were provided Fisher Scientific (Loughborough, Leicestershire, UK). Visking dialysis membrane tubing (MWCO of 12–14 kDa), agar and sodium hyaluronate (1.8 MDa) were obtained from Medicell International Ltd. (London, UK), Fluka Analytical (Gillingham, Dorset, UK) and Aston Chemicals (Aylesbury, UK) respectively. PD-10, Nap-10 and HiTrap™ SPHP columns were obtained from GE Healthcare (Amersham, UK). Viva 6 centrifugal concentrators (MWCO 10 kDa) were purchased from Generon (Berkshire, UK). Novex sharp pre-stained standard marker, NuPage® LDS sample buffer, 4-12% Bis-Tris polyacrylamide gels, 1.0 mm x 10 well and NuPage® MOPS running buffer were supplied from Life Technologies

(Northumberland, UK). Deuterated chloroform, $CDCl_3$ (Cambridge Isotope Laboratories, Andover, UK) was used for nuclear magnetic resonance (NMR).

Instrumentation

A 16-channel Ismatec peristaltic pump (Michael Smith Engineers Ltd., Woking, Surrey, UK) was used to maintain fluid flow through the PK-Eye. High performance liquid chromatography (HPLC) was conducted using an Agilent 1200 series equipped with Chemstation software using a Zorbax GF-250 column (Agilent, Wokingham, Berkshire, UK). UV measurements were performed using a Hitachi U-2800A spectrometer using Quartz cuvettes (Starna Scientific Ltd) with a wavelength range of 200 nm to 800 nm and a Wallac Victor2 1420 plate reader. Scanning electron microscopy (SEM) was achieved using a QuantaTM 200F instrument (FEI Quanta200 FEGESEM, Eindhoven, The Netherlands). Different scanning calorimetry (DSC) experiments were performed on DSC Q2000 (TA instruments, Waters, LLC) with TA Instruments Universal Analysis 2000 software. A VIRTIS-Advantage freeze-dryer was used for freeze-drying. SDS-PAGE was conducted using XcellSureLock gel electrophoresis tank (EI0001) and power supply (Life Technologies, Northumberland, UK). The IEX system had a UV detector (Jasco UV-1570) and HPLC pump (Jasco PU-980 Intelligent) with Azur software.

NIPAAM gel preparation.

Bevacizumab (0.5 or 1.0 mL of 25.0 mg/mL solution) was gently mixed with NIPAAM (40.0 mg, 3.5×10^{-4} moles) and APS (4.0 mg, 1.7×10^{-5} moles, 0.048 equiv.) for 10-15 mins. PEGDA (Mn 700, δ: 1.12 g/mL, 25°C) was added in one of the following amounts: 4 (6.4×10^{-6} moles), 8 (1.3×10^{-5} moles) and 12 µL (1.9×10^{-5} moles) and the reaction mixtures were gently vortexed. TEMED (50 µL, δ: 0.775 g/mL, 20°C, 3.3×10^{-4} moles) was then added and vortexed for 15-20 s. The mixture was stored in the fridge for 24 hours at 4°C. To wash, phosphate buffered saline (PBS, pH 7.4, 5.0 mL) was added to the gelled product and gently mixed for 5-10 mins. This process

was repeated 4 times using a total of 20.0 mL of PBS. Unwashed gels were used directly after polymerisation. Protein loading of the gel was determined by HPLC (280 nm).

Preparation of bevacizumab loaded NIPAAM gels.

NIPAAM (40 mg, 3.5×10^{-4} moles) and APS (4.0 mg, 1.7×10^{-5} moles, 0.048 equiv.) were dissolved in deionised water (1.0 mL) at RT (25°C). The contents were mixed for 10 mins (magnetic stir bar) until a clear solution was formed. Different PEGDA concentrations (Mn 700, δ: 1.12 g/mL, 25°C) were screened in the range of (0.018 to 0.091 equiv. to NIPAAM). The amounts of PEGDA used in separate NIPAAM polymerisation reactions were 4 (6.4×10^{-6} moles), 8 (1.3×10^{-5} moles), 12 (1.9×10^{-5} moles), 15 (2.4×10^{-5} moles) or 20 µL (3.2×10^{-5} moles) with increasing PEGDA used to increase the cross-link density of the NIPAAM gel. The reaction mixtures were vortexed for 10 min and then TEMED (δ: 0.775 g/mL, 20°C, 3.3×10^{-4} moles) was added. The mixture was again vortexed (~15-20 s) and then placed in a refrigerator (4°C, 24 h).

The hydrogel was then freeze-dried prior to characterisation. All samples for freeze-drying were frozen in dry ice and then transferred to the freeze-drier at -40°C with a condenser temperature of -60°C. The vacuum pressure was maintained less than 200 mBar. The primary freeze-drying step was at -20°C for 48 hours. The temperature was increased to 20°C for 2 hours before opening the freeze-drier.

Preparation of PEG_{10}-Fab_{rani} loaded NIPAAM hydrogels.

The PEGylation reagent **1** used for conjugation was prepared as previously reported.[81-83] The conjugation buffer consisted of sodium phosphate monobasic (20.0 mM) and EDTA (10.0 mM) in distilled water (250.0 mL, Type I, 18.2 mΩ) and the pH was adjusting to 7.4. The prepared buffer was purged with argon before use. A solution of ranibizumab (Fab_{rani}, 0.1 mL of 10.0 mg/mL) was prepared in conjugation buffer and it was reduced with DTT (5 mM, pH 7.4) for 30 mins at RT

(~25°C). The reduced Fab_{rani} was buffer exchanged to pH 7.6 using a PD-10 column. The reduced Fab_{rani} was found in the first 2.0 mL of the eluted buffer. PEG_{10} *bis*-sulfone **1** was added to the reduced Fab_{rani} at a PEG reagent:Fab_{rani} ratio of 2:1 (pH 7.6) and the conjugation mixture was incubated under an argon atmosphere for 5 hours at RT.

PEG_{10}-Fab_{rani} was then purified by ion exchange chromatography. Buffer A (sodium acetate trihydrate, 50.0 mM) and buffer B (sodium acetate trihydrate, 50 mM and sodium chloride 500 mM) were prepared in distilled water (500.0 mL, Type I, 18.2 mΩ resistance) and adjusted to pH 4.0. The buffers were filtered prior to connecting them to the HPLC with a 0.45 µm with a Millipore filter flask fitted with cellulose nitrate membrane. A Nap-10 column was washed and equilibrated with buffer A. The conjugate (1.0 mL) was buffer exchanged with buffer A (1.5 mL) to give the protein a charge that would allow binding to the column. The flow-through was collected and loaded to the SPHP column. A linear gradient was used by first eluting 100% buffer A for 10 minutes, then gradually eluting 100% buffer B over a 30 minute period (total run time: 40 mins). The column effluent was monitored by UV (280 nm). Fractions (~1.0 mL) were collected and analysed by SDS-PAGE to isolate PEG_{10}-Fab_{rani}. The PEG_{10}-Fab_{rani} fractions were pooled and concentrated with viva-spin (MWCO 10 kDa) to ~1.0 mL and the UV absorbance was recorded at 280 nm. The conjugate was then stabilised by the addition of sodium triacetoxyborohydride (STAB, 50 mM) dissolved in DMSO at 4°C for 1.5 hours. The crude reaction mixture was buffer exchanged with a PD-10 column into 50 mM PBS, pH 7.4.

PEG_{10}-Fab_{rani} (0.5-2.0 mg) was gently mixed (magnetic stir bar) with NIPAAM (40 mg, 3.5×10^{-4} moles) and APS (4.0 mg, 1.7×10^{-5} moles) for 3-4 hours (RT). PEGDA i.e. 8 µL (δ: 1.12 g/mL, 25°C, 1.3×10^{-5} moles) was then added and vortexed. TEMED (50 µL, δ: 0.775 g/mL, 20°C, 3.3×10^{-4} moles) was added and vortexed. The mixture was incubated in the fridge for 24 hours at 4°C.

Determination of volume phase transition temperature (VPTT)

The VPTT was measured using differential scanning calorimetry (DSC) at 2°C/min from 20 to 50°C. Calibration with Indium (Tm = 156.6, ∆Hf =28.71 J/g) was performed according to the manufacturer instructions. Nitrogen was used as purge gas with a flow rate of 40.0 mL/min for all the experiments. The onset temperature of the DSC endothermic peak was considered as the VPTT.

Determination of swelling ratio (SR) and water retention (WR)

Freeze dried hydrogel samples were weighed (*Wd*) and rehydrated in deionised water for approximately 48 hours to ensure full hydration of the hydrogel. Hydrogels were allowed to reach equilibrium swelling at three different temperatures (25, 37 and 48°C). The fully hydrated samples were then removed and weighed to measure their weight at equilibrium with water (*We*). Excess water was removed from the sample by tapping the surface carefully with filter paper before reweighing. A gravimetric method was used to measure the swelling ratio (*Q*) of the prepared hydrogels with Equation 1.

$$Q = \frac{(We - Wd)}{Wd} \qquad \textbf{Equation 1}$$

Water retention percentage (WR%) was measured using the gravimetric method at 50°C. Freeze-dried hydrogel samples were weighed (*Wd*) and were fully hydrated at RT (~25°C) in deionised water (10.0 mL) for 48 hours. The fully hydrated gels were weighed (*We*) and quickly transferred to pre-heated water at 50°C in an incubator. The samples were weighed at pre-determined time intervals. The samples were removed from the incubator, quickly weighed (*Wt*) and returned back to the incubator before each measurement. WR% was calculated for each time point according to Equation 2.

$$WR\% = 100 \times \frac{(Wt - Wd)}{We} \qquad \textbf{Equation 2}$$

Scanning electron microscopy (SEM).

Samples were cut and adhered onto aluminium SEM stubs using carbon-coated double-sided tape prior to SEM analysis. The samples were then sputter coated with gold prior to imaging to make them electrically conductive.

In vitro release studies using the PK-Eye.

The *in vitro* PK-Eye is a two-compartment model comprised of anterior (0.2 mL) and posterior (4.2 mL) cavities separated with a washer and Visking membrane (MWCO 12-14 kDa). For PEG_{10}-Fab_{rani} studies, a solution of Tween 20 (30%) in distilled water was first prepared. Freshly cut Visking membranes were incubated in the Tween 20 solution for ~12 hours at 37°C. The membranes were then rinsed gently with distilled water and the membranes were fitted with the washer and integrated within the model. The control in this experiment was the membrane not treated with Tween 20.

The inlet port of the PK-Eye was connected to a peristaltic pump with a flow of 2.0 µL/min. One outlet port is present in the anterior cavity for continuous sampling. An injection port is present in both cavities (diameter: 2.0-3.0 mm) to allow formulation administration into the model. Prior to each experiment, the PK-Eye was unscrewed and a fresh Visking membrane was incorporated. The models were assembled and the anterior cavity was filled with PBS, pH 7.4, whereas the posterior cavity was filled with simulated vitreous or PBS. The models were immersed in a preheated oil bath adjusted to 37°C for 2 hours to equilibrate prior to the release studies. Temperature was maintained using a probe connected to the hotplate heater.

To prepare simulated vitreous with a dynamic viscosity of 0.6 Pa.s,[39] which is similar to the human vitreous viscosity (~0.5 Pa.s).[89] Agar (0.4 g) and hyaluronic acid (HA) (0.5 g) were separately mixed in 100 mL of boiled water.[90] The agar solution was boiled to completely solubilise the agar. After boiling, the hot agar solution was mixed with HA and stirred to give a homogenous mixture to which a few

drops of 0.02% sodium azide were added. The solution was left to cool for 24 hours at RT to form a gel-like consistency.

The following formulations were injected to the posterior cavity of the PK-Eye via a 23 G needle: (i) injection form of bevacizumab (Avastin®, 25 mg/mL), 1.25 (50 µL), 2.5 (100 µL) and 5.0 mg (200 µL); (ii) bevacizumab (2.5 mg, 100 µL) loaded NIPAAM gels with PEGDA (4, 8 and 12 µL); (iii) Injection form of PEG_{10}-Fab_{rani}, 0.6 (50 µL), 1.0, (100 µL) and 2.0 mg (200 µL) and (iv) PEG_{10}-Fab_{rani} (2.0 mg, 200 µL) loaded NIPAAM gels with PEGDA (8 µL). Samples were collected from the anterior cavity and quantified by HPLC (280 nm).

Protein quantification by high performance liquid chromatography (HPLC)

Protein concentration was determined by HPLC with an Agilent Zorbax GF-250 column fitted with a guard column. The mobile phase was PBS, pH 7.4 previously purged with argon and sonicated. A wavelength of 280 nm was adjusted with a run time of 12 minutes. The injection volume was 100 µL with a flow rate of 1.0 mL/min. A calibration curve was made with a 0.0019-1.0 mg/mL of protein in PBS, pH 7.4. Bevacizumab and ranibizumab had a reported R^2 value of 0.996 and 0.987 respectively. A retention time of approximately 2.3 mins was observed.

Data analysis

All results are presented as the mean (n=3) and standard deviation (± STD), and data were plotted using OriginPro 9.1 (software, Origin lab cooperation, USA). Half-life ($t_{1/2}$) values were calculated according to the best fitting model in OriginPro. First-order kinetic rate constants (k) were derived from the mono-exponential curve and $t_{1/2}$ was calculated using the equation: $0.693/k$. The rate constants (k) of zero-order release profiles were calculated as concentration-time and $t_{1/2}$ was calculated from initial concentration [A] using $[A]/2k$. The analysis of variance (one-way and repeated measure ANOVA) with Tukey's post hoc test was conducted to evaluate differences between the experimental data (mean values) using OriginPro 9.1 and IBM SPSS

statistics 23. Probability values less than 0.05 ($p<0.05$) were considered as indicative of statistically significant differences.

Acknowledgements

We are grateful for funding from the National Institute of Health Research (NIHR) Biomedical Research Centre at Moorfields Eye Hospital NHS Foundation Trust and UCL Institute of Ophthalmology, Moorfields Special Trustees, the Helen Hamlyn Trust (in memory of Paul Hamlyn), Medical Research Council, Fight for Sight and the Michael and Ilse Katz foundation. S.A. gratefully acknowledges funding from the UCL Overseas Research Student Fund and A.A.S. is grateful for funding from the Iraqi Government.

References

[1] S. Mitragotri, P. Burke, R. Langer, Overcoming the challenges in administering biopharmaceuticals: formulation and delivery strategies, *Nat. Rev. Drug Discovery*, **2014**, *13*, 655.

[2] V. S. Jatav, H. Singh, S. K. Singh, Recent trends on hydrogel in human body, *Int. J. Res. Pharm. Biomed. Sci*, **2011**, *2*, 442.

[3] C. Gong, T. Qi, X. Wei, Y. Qu, Q. Wu, F. Luo, Z. Qian, Thermosensitive Polymeric Hydrogels As Drug Delivery Systems, *Curr. Med. Chem.*, **2013**, *20*, 79.

[4] Y. Qiu, K. Park, Environment-sensitive hydrogels for drug delivery, *Adv. Drug Delivery Rev.*, **2001**, *53*, 321.

[5] B. M. Rauck, T. R. Friberg, C. A. Medina Mendez, D. Park, V. Shah, R. A. Bilonick, Y. Wang, Biocompatible reverse thermal gel sustains the release of intravitreal bevacizumab in vivo, *Invest. Ophthalmol. Vis. Sci.*, **2013**, *55*, 469.

[6] Y.S. Hwang, P.R. Chiang, W.H. Hong, C.C. Chiao, I. M. Chu, G.H. Hsiue, C.R. Shen, Study in vivo intraocular biocompatibility of in situ gelation hydrogels: poly(2-ethyl oxazoline)-block-poly(ε -caprolactone)-block-poly(2-ethyl oxazoline) copolymer, matrigel and pluronic F127, *PLoS One*, **2013**, *8*, e67495.

[7] A. Prasannan, H.C. Tsai, Y.S. Chen, G.H. Hsiue, A thermally triggered in situ hydrogel from poly(acrylic acid-co-N-isopropylacrylamide) for controlled release of anti-glaucoma drugs, *J. Mater. Chem. B*, **2014**, *2*, 1988.

[8] U. B. Kompella, H. F. Edelhauser, *Drug Product Development for the Back of the Eye*, in *AAPS Advances in the Pharmaceutical Sciences Series*. 2011, Springer US: Boston, MA.

[9] P. Adamson, T. Wilde, E. Dobrzynski, C. Sychterz, R. Polsky, E. Kurali, R. Haworth, C.M. Tang, J. Korczynska, F. Cook, I. Papanicolaou, L. Tsikna, C. Roberts, Z. Hughes-Thomas, J. Walford, D. Gibson, J. Warrack, J. Smal, R. Verrijk, P. E. Miller, T. M. Nork, J. Prusakiewicz, T. Streit, S. Sorden, C. Struble, B. Christian, I. R. Catchpole, Single ocular injection of a sustained-release anti -VEGF delivers 6 months pharmacokinetics and ef fi cacy in a primate laser CNV model, *J. Controlled Release*, **2016**, *244*, 1.

[10] T. R. Thrimawithana, S. Young, C. R. Bunt, Drug delivery to the posterior segment of the eye, *Drug Discovery Today*, **2011**, *16*, 270.

[11] K. Radhakrishnan, N. Sonali, M. Moreno, J. Nirmal, A. A. Fernandez, S. Venkatraman, R. Agrawal, Protein delivery to the back of the eye: barriers, carriers and stability of anti-VEGF proteins, *Drug Discovery Today*, **2017**, *22*, 416.

[12] V. Delplace, S. Payne, M. Shoichet, Delivery strategies for treatment of age-related ocular diseases: From a biological understanding to biomaterial solutions, *J. Control. Release*, **2015**, *219*, 652.

[13] J. J. Kang-Mieler, C. R. Osswald, W. F. Mieler, Advances in ocular drug delivery: emphasis on the posterior segment, *Expert Opin. Drug Delivery*, **2014**, *11*, 1647.

[14] Y. Perrie, R.K.S. Badhan, D. J. Kirby, The impact of ageing on the barriers to drug delivery, *J. Control. Release*, **2012**, *161*, 389.

[15] M. Cabrera, S. Yeh, T. A. Albini, Sustained-Release Corticosteroid Options, *J. Ophthalmol.*, **2014**, *2014*, 1.

[16] R. Baid, P. Tyagi, S. A. Durazo, U. B. Kompella, *Protein Drug Delivery and Formulation Development*. 2011. p. 409.

[17] Y. Yu, L.C.M. Lau, A. C.Y. Lo, Y. Chau, Injectable Chemically Crosslinked Hydrogel for the Controlled Release of Bevacizumab in Vitreous: A 6-Month In Vivo Study, *Translational Vision Science & Technology*, **2015**, *4*, 5.

[18] J. Shi, P. Kantoff, R. Wooster, O. Farokhzad, Cancer nanomedicine: progress, challenges and opportunities, *Nat. Rev. Cancer*, **2017**, *17*, 20.

[19] X. Rong, W. Yuan, Y. Lu, X. Mo, Safety evaluation of poly(lactic-co-glycolic acid)/poly(lactic-acid) microspheres through intravitreal injection in rabbits, *Int. J. Nanomed.*, **2014**, *9*, 3057.

[20] N. Su, Y. Li, T. Xu, L. Li, J.S.W. Kwong, H. Du, K. Ren, Q. Li, J. Li, X. Sun, S. Li, H. Tian, Exenatide in obese or overweight patients without diabetes: A systematic review and meta-analyses of randomized controlled trials, *Int. J. Cardiol.*, **2016**, *219*, 293.

[21] P. Grass, P. Marbach, C. BrunsI. Lancranjan, Sandostatin® LAR® (microencapsulated octreotide acetate) in acromegaly: Pharmacokinetic and pharmacodynamic relationships, *Metabolism*, **1996**, *45*, 27.

[22] M. S. Gordon, T. W. Kinlock, F. J. Vocci, T. T. Fitzgerald, A. MemisogluB. Silverman, A Phase 4, Pilot, Open-Label Study of VIVITROL (Extended-Release Naltrexone XR-NTX) for Prisoners, *J. Subst. Abuse Treat.*, **2015**, *59*, 52.

[23] E. J. De Waal, W. Roosen, P. Vinken, J. Vandenberghe, P. SterkensL. Lammens, Mechanistic investigations on the etiology of Risperdal® Consta®-induced bone changes in female Wistar Hannover rats, *Toxicology*, **2012**, *299*, 90.

[24] F. Sousa, A. Cruz, P. Fonte, I. M. Pinto, M. T. Neves-Petersen, B. Sarmento, A new paradigm for antiangiogenic therapy through controlled release of bevacizumab from PLGA nanoparticles, *Sci. Rep.*, **2017**, *7*, 3736.

[25] H. K. Kim, T. G. Park, Microencapsulation of human growth hormone within biodegradable polyester microspheres: Protein aggregation stability and incomplete release mechanism, *Biotechnol. Bioeng.*, **1999**, *65*, 659.

[26] D. S. Pisal, M. P. Kosloski, S. V. BaluIyer, Delivery of therapeutic proteins, *J. Pharm. Sci.*, **2010**, *99*, 2557.

[27] K. Park, Ocular microparticle formulations for 6-month delivery of anti-VEGF, *J. Controlled Release*, **2016**, *244*, 136.

[28] R. R. Joseph, S. S. Venkatraman, Drug delivery to the eye: what benefits do nanocarriers offer?, *Nanomedicine*, **2017**, *12*, 683.

[29] J. Helzner *Genentech acquires developer of sustained-release implants.* Retinal Physician, 2017.

[30] C. R. Osswald, J. J. Kang-Mieler, Controlled and Extended In Vitro Release of Bioactive Anti-Vascular Endothelial Growth Factors from a Microsphere-Hydrogel Drug Delivery System, *Curr. Eye Res.*, **2016**, *41*, 1216.

[31] S. Kirchhof, A. M. Goepferich, F. P. Brandl, Hydrogels in ophthalmic applications, *Eur. J. Pharm. Biopharm.*, **2015**, *95*, 227.

[32] J. Barar, A. Aghanejad, M. Fathi, Y. Omidi, Advanced drug delivery and targeting technologies for the ocular diseases, *BioImpacts*, **2016**, *6*, 49.

[33] P. W. Drapala, E. M. Brey, W. F. Mieler, D. C. Venerus, J. J. Kang Derwent, V. H. Pérez-Luna, Role of Thermo-responsiveness and Poly(ethylene glycol)

Diacrylate Cross-link Density on Protein Release from Poly(N-isopropylacrylamide) Hydrogels, *J. Biomater. Sci. Polym. Ed.*, **2011**, *22*, 59.

[34] J. J. Kang Derwent, W. F. Mieler, Thermoresponsive hydrogels as a new ocular drug delivery platform to the posterior segment of the eye, *Trans. Am. Ophthalmol. Soc.*, **2008**, *106*, 206.

[35] P. W. Drapala, B. Jiang, Y. C. Chiu, W. F. Mieler, E. M. Brey, J. J. Kang-Mieler, V. H. Pérez-Luna, The effect of glutathione as chain transfer agent in PNIPAAm-based thermo-responsive hydrogels for controlled release of proteins, *Pharm. Res.*, **2014**, *31*, 742.

[36] X. Li, W. Wu, W. Liu, Synthesis and properties of thermo-responsive guar gum/poly(N-isopropylacrylamide) interpenetrating polymer network hydrogels, *Carbohydr. Polym.*, **2008**, *71*, 394.

[37] S. B. Turturro, M. J. Guthrie, A. A. Appel, P. W. Drapala, E. M. Brey, V. H. Pérez-Luna, W. F. Mieler, J. J. Kang-Mieler, The effects of cross-linked thermo-responsive PNIPAAm-based hydrogel injection on retinal function, *Biomaterials*, **2011**, *32*, 3620.

[38] S. Awwad, R.M. Day, P.T. Khaw, S. Brocchini, H. M. Fadda, Sustained release ophthalmic dexamethasone: In vitro in vivo correlations derived from the PK-Eye, *Int. J. Pharm.*, **2017**, *522*, 119.

[39] S. Awwad, A. Lockwood, S. Brocchini, P. T. Khaw, The PK-Eye: A Novel *In Vitro* Ocular Flow Model for Use in Preclinical Drug Development, *J. Pharm. Sci.*, **2015**, *104*, 3330.

[40] A. Baskakova, S. Awwad, J. Q. Jiménez, H. Gill, O. Novikov, P. T. Khaw, S. Brocchini, E. Zhilyakova, G. R. Williams, Electrospun formulations of acyclovir, ciprofloxacin and cyanocobalamin for ocular drug delivery, *Int. J. Pharm.*, **2016**, *502*, 208.

[41] J. Kang Derwent, W. Mieler, Thermoresponsive hydrogels as a new ocular drug delivery platform to the posterior segment of the eye., *Trans. Am. Ophthalmol. Soc.*, **2008**, *106*, 206.

[42] X.Z. Zhang, Y.Y. Yang, T.S. Chung, K.X. Ma, Preparation and characterization of fast response macroporous poly(N-isopropylacrylamide) hydrogels, *Langmuir*, **2001**, *17*, 6094.

[43] M. Elshout, M. I. Van Der Reis, C.A.B. Webers, J. S. G. Schouten, The cost-utility of aflibercept for the treatment of age-related macular degeneration compared to bevacizumab and ranibizumab and the influence of model parameters, *Graefe's Archive for Clinical and Experimental Ophthalmology*, **2014**, *252*, 1911.

[44] T. Q. Kwong, M. Mohamed, Anti Vascular Endothelial Growth Factor therapies in Ophthalmology: Current Use, Controversies and the Future, *Br. J. Clin. Pharmacol.*, **2014**, 1.

[45] U. Chakravarthy, S. P. Harding, C. A. Rogers, S. M. Downes, A. J. Lotery, S. Wordsworth, B. C. Reeves, Ranibizumab versus bevacizumab to treat neovascular age-related macular degeneration: One-year findings from the IVAN randomized trial, *Ophthalmology*, **2012**, *119*, 1399.

[46] R. Brubaker, The flow of aqueous humor in the human eye., *Trans. Am. Ophthalmol. Soc.*, **1982**, *80*, 391.

[47] C. Toris, M. Yablonski, Y. Wang, C. Camras, Aqueous humor dynamics in the aging human eye., *Am. J. Ophthalmol.*, **1999**, *127*, 407.

[48] D. Maurice, Review: Practical issues in intravitreal drug delivery., *J. Ocul. Pharmacol. Ther.*, **2001**, *17*, 393.

[49] J. Siggers, C. Ethier, Fluid mechanics of the eye., *Annu. Rev. Fluid Mech.*, **2012**, *44*, 347.

[50] V. Agrahari, A. Mandal, V. Agrahari, H. Trinh, M. Joseph, A. Ray, H. Hadji, R. Mitra, D. Pal, M. Ak, A comprehensive insight on ocular pharmacokinetics, *Drug Deliv. and Transl. Res.*, **2017**, *6*, 735.

[51] Y. Vugmeyster, X. Xu, F.P. Theil, L. A. Khawli, M. W. Leach, Pharmacokinetics and toxicology of therapeutic proteins: advances and challenges, *World J. Biol. Chem.*, **2012**, *3*, 73.

[52] V. Brinks, W. Jiskoot, H. Schellekens, Immunogenicity of therapeutic proteins: the use of animal models, *Pharm. Res.*, **2011**, *28*, 2379.

[53] S. Tamilvanan, N. L. Raja, B. Sa, S. K. Basu, Clinical concerns of immunogenicity produced at cellular levels by biopharmaceuticals following their parenteral administration into human body, *J. Drug Target.*, **2010**, *18*, 489.

[54] W. Wang, S. K. Singh, N. Li, M. R. Toler, K. R. King, S. Nema, Immunogenicity of protein aggregates—concerns and realities, *Int. J. Pharm.*, **2012**, *431*, 1.

[55] K. S. Brinch, N. Frimodt-Møller, N. Høiby, H.-H. Kristensen, Influence of antidrug antibodies on plectasin efficacy and pharmacokinetics, *Antimicrob. Agents Chemother.*, **2009**, *53*, 4794.

[56] A. Laude, L. E. Tan, C. G. Wilson, G. Lascaratos, M. Elashry, T. Aslam, N. Patton, B. Dhillon, Intravitreal therapy for neovascular age-related macular degeneration and inter-individual variations in vitreous pharmacokinetics, *Prog. Retinal Eye Res.*, **2010**, *29*, 466.

[57] B. G. Short, Safety evaluation of ocular drug delivery formulations: techniques and practical considerations, *Toxicol. Pathol.*, **2008**, *36*, 49.

[58] T. U. Krohne, F. G. Holz, C. H. Meyer, Pharmacokinetics of intravitreally administered VEGF inhibitors, *Der Ophthalmologe*, **2014**, *111*, 113.

[59] C. H. Meyer, T. U. Krohne, F. G. Holz, Intraocular pharmacokinetics after a single intravitreal injection of 1.5 mg versus 3.0 mg of bevacizumab in humans, *Retina (Philadelphia, Pa.)*, **2011**, *31*, 1877.

[60] Q. Zhu, F. Ziemssen, S. Henke-Fahle, O. Tatar, P. Szurman, S. Aisenbrey, N. Schneiderhan-Marra, X. Xu, S. Grisanti, Vitreous levels of bevacizumab and vascular endothelial growth factor-A in patients with choroidal neovascularization, *Ophthalmology*, **2008**, *115*, 1750.

[61] P. M. Beer, S. J. Wong, A. M. Hammad, N. S. Falk, M. R. O'malley, S. Khan, Vitreous levels of unbound bevacizumab and unbound vascular endothelial growth factor in two patients, *Retina*, **2006**, *26*, 871.

[62] A. Penedones, D. Mendes, C. Alves, F. Batel-Marques, Safety monitoring of ophthalmic biologics: a systematic review of pre- and postmarketing safety data, *J. Ocul. Pharmacol. Ther.*, **2014**, *30*, 729.

[63] Y. G. Yu, Y. Xu, H. Ning, S. S. Zhang, Swelling behaviors of thermoresponsive hydrogels cross-linked with acryloyloxyethylaminopolysuccinimide, *Colloid. Polym. Sci.*, **2008**, *286*, 1165.

[64] C. Erbil, E. Kazancıoğlu, N. Uyanık, Synthesis, characterization and thermoreversible behaviours of poly(dimethyl siloxane)/poly(N-isopropyl acrylamide) semi-interpenetrating networks, *Eur. Polym. J.*, **2004**, *40*, 1145.

[65] A. T. Gökçeören, B. F. Şenkal, C. Erbil, Effect of crosslinker structure and crosslinker/monomer ratio on network parameters and thermodynamic

properties of Poly (N-isopropylacrylamide) hydrogels, *J. Polym. Res.*, **2014**, *21*, 1.

[66] H. S. Samanta, S. K. Ray, Synthesis, characterization, swelling and drug release behavior of semi-interpenetrating network hydrogels of sodium alginate and polyacrylamide, *Carbohydr. Polym.*, **2014**, *99*, 666.

[67] Y. Kaneko, S. Nakamura, K. Sakai, T. Aoyagi, A. Kikuchi, Y. Sakurai, T. Okano, Rapid deswelling response of poly(N-isopropylacrylamide) hydrogels by the formation of water release channels using poly(ethylene oxide) graft chains, *Macromolecules*, **1998**, *31*, 6099.

[68] P. N. Bishop, D. F. Holmes, K. E. Kadler, D. Mcleod, K. J. Bos, Age-related changes on the surface of vitreous collagen fibrils, *Invest. Ophthalmol. Vis. Sci.*, **2004**, *45*, 1041.

[69] E. Moisseiev, M. Waisbourd, E. Ben-Artsi, E. Levinger, A. Barak, T. Daniels, K. Csaky, A. LoewensteinI. S. Barequet, Pharmacokinetics of bevacizumab after topical and intravitreal administration in human eyes, *Graefe's Archive for Clinical and Experimental Ophthalmology*, **2014**, *252*, 331.

[70] T. Nakajima, H. Furukawa, Y. Tanaka, T. Kurokawa, Y. OsadaJ. P. Gong, True chemical structure of double network hydrogels, *Macromolecules*, **2009**, *42*, 2184.

[71] C. J. Fee, J. M. V. Alstine, Prediction of the Viscosity Radius and the Size Exclusion Chromatography Behavior of PEGylated Proteins, *Bioconjugate Chem.*, **2004**, *15*, 1304.

[72] Y. Lu, S. E. Harding, A. Turner, B. Smith, D. S. Athwal, N. Grossmann, K. G. Davis, A. J. Rowe, J. Gu, Effect of PEGylation on the Solution Conformation of Antibody Fragments, *J. Pharm. Sci.*, **2008**, *97*, 2062.

[73] E. Vernet, G. Popa, I. Pozdnyakova, J. E. Rasmussen, H. Grohganz, L. Giehm, M. H. Jensen, H. Wang, B. Plesner, H. M. Nielsen, K. J. Jensen, J. Berthelsen, M. V. D. Weert, Large-Scale Biophysical Evaluation of Protein PEGylation E ff ects: In Vitro Properties of 61 Protein Entities, *Mol. Pharm.*, **2016**, *13*, 1587.

[74] G. Cattani, L. Vogeley, P. B. Crowley, Structure of a PEGylated protein reveals a highly porous double-helical assembly, *Nat. Chem.*, **2015**, *7*, 823.

[75] T. M. Aminabhavi, M. N. Nadagouda, U. A. More, S. D. Joshi, V. H. Kulkarni, M. N. Noolvi, P. V. Kulkarni, Controlled release of therapeutics using interpenetrating polymeric networks, *Expert Opin. Drug Delivery*, **2014**, *12*, 669.

[76] E. M. Amo, A.K. Rimpelä, E. Heikkinen, O. K. Kari, E. Ramsay, T. Lajunen, M. Schmitt, L. Pelkonen, M. Bhattacharya, D. Richardson, A. Subrizi, T. Turunen, M. Reinisalo, J. Itkonen, E. Toropainen, M. Casteleijn, H. Kidron, M. Antopolsky, M. Ruponen, A. Urtti, Pharmacokinetic aspects of retinal drug delivery, *Prog. Retin. Eye Res.*, **2017**, *57*, 134.

[77] W. Shatz, P. E. Hass, M. Mathieu, H. S. Kim, K. Leach, M. Zhou, Y. Crawford, A. Shen, K. Wang, D. P. Chang, Contribution of antibody hydrodynamic size to vitreal clearance revealed through rabbit studies using a species-matched fab, *Mol. Pharmaceutics*, **2016**, *13*, 2996.

[78] H. Khalili, A. Godwin, J.W. Choi, R. Lever, S. Brocchini, Comparative binding of disulfide-bridged PEG-Fabs, *Bioconjugate Chem.*, **2012**, *23*, 2262.

[79] N. Goel, S. Stephens, Certolizumab pegol, *mAbs*, **2010**, *2*, 137.

[80] W. Shatz, P. E. Hass, M. Mathieu, H. S. Kim, K. Leach, M. Zhou, Y. Crawford, A. Shen, K. Wang, D. P. Chang, M. Maia, S. R. Crowell, L.

Dickmann, J. M. Scheer, R. F. Kelley, Contribution of Antibody Hydrodynamic Size to Vitreal Clearance Revealed through Rabbit Studies Using a Species-Matched Fab, *Mol. Pharm.*, **2016**, *13*, acs.molpharmaceut.6b00345.

[81] S. Brocchini, A. Godwin, S. Balan, J.W. Choi, M. Zloh, S. Shaunak, Disulfide bridge based PEGylation of proteins, *Adv. Drug Delivery Rev.*, **2008**, *60*, 3.

[82] S. Brocchini, S. Balan, A. Godwin, J.W. Choi, M. Zloh, S. Shaunak, PEGylation of native disulfide bonds in proteins, *Nat. Protoc.*, **2006**, *1*, 2241.

[83] S. Shaunak, A. Godwin, J. W. Choi, S. Balan, E. Pedone, D. Vijayarangam, S. Heidelberger, I. Teo, M. Zloh, S. Brocchini, Site-specific PEGylation of native disulfide bonds in therapeutic proteins., *Nat. Chem. Bio.*, **2006**, 312.

[84] S. Balan, J.-W. Choi, A. Godwin, I. Teo, C. M. Laborde, S. Heidelberger, M. Zloh, S. Shaunak, S. Brocchini, Site-Specific PEGylation of Protein Disulfide Bonds Using a Three-Carbon Bridge, *Bioconjug. Chem.*, **2007**, *18*, 61.

[85] T. U. Krohne, N. Eter, F. G. Holz, C. H. Meyer, Intraocular pharmacokinetics of bevacizumab after a single intravitreal injection in humans, *Am. J. Ophthalmol.*, **2008**, *146*, 508.

[86] L. Xu, T. Lu, L. Tuomi, N. Jumbe, J. Lu, S. Eppler, P. Kuebler, L. A. Damico-Beyer, A. Joshi, Pharmacokinetics of ranibizumab in patients with neovascular age-related macular degeneration: A population approach, *Invest. Ophthalmol. Vis. Sci.*, **2013**, *54*, 1616.

[87] E. W. M. Ng, D. T. Shima, P. Calias, E. T. Cunningham, D. R. Guyer, A. P. Adamis, Pegaptanib, a targeted anti-VEGF aptamer for ocular vascular disease, *Nat. Rev. Drug Discovery*, **2006**, *5*, 123.

[88] A. S. Basile, M. Hutmacher, D. Nickens, Population Pharmacokinetics of Pegaptanib in Patients With Neovascular, Age-Related Macular Degeneration, *J. Clin. Pharmacol.*, **2012**, *52*, 1186.

[89] N. Soman, R. Banerjee, Artificial vitreous replacements, *Biomed. Mater. Eng.*, **2003**, *13*, 59.

[90] M. Kummer, J. Abbott, S. Dinser, B. Nelson, Artificial vitreous humor for in vitro experiments, *Conf. Proc. Int. Conf. IEEE Eng. Med. Biol. Soc.*, **2007**, 6407.